



Contents lists available at ScienceDirect

Journal of King Saud University – Computer and Information Sciences

journal homepage: www.sciencedirect.com

An effective robust and imperceptible blind color image watermarking using WHT

K. Prabha^{a,*}, I. Shatheesh Sam^b^a Research Scholar, Register Number: 1721311262014, Department of Computer Science, Nesamony Memorial Christian College, Marthandam affiliated to Manonmaniam Sundaranar, University, Abishekapatti, Tirunelveli 627 012, Tamil Nadu, India^b Associate Professor, Department of PG Computer Science, Nesamony Memorial Christian College, Marthandam affiliated to Manonmaniam Sundaranar, University, Abishekapatti, Tirunelveli 627 012, Tamil Nadu, India

ARTICLE INFO

Article history:

Received 27 September 2019

Revised 24 January 2020

Accepted 2 April 2020

Available online xxxx

Keywords:

Walsh Hadamard Transform

Blind watermarking

Color image watermarking

Non-overlapping blocks

Weighted Peak Signal-to-Noise Ratio

ABSTRACT

Digital image watermarking is the most widely used recognized approach to protect data against piracy. This paper proposes a new blind color image watermarking based on the Walsh Hadamard Transform (WHT). The proposed method subdivides the image into 4×4 non-overlapping blocks, which are then transformed using WHT. The color image watermark is embedded in the third and fourth-row WHT coefficients using the proposed technique as a slight change in those rows may not profoundly affect the visual quality of an image. Then the difference of the third and fourth row WHT coefficients of the watermarked image is obtained. The watermark information is extracted using the attained difference value. The performance evaluation of the proposed scheme outperforms in terms of embedding capacity, Peak Signal-to-Noise Ratio (PSNR), Weighted Peak Signal-to-Noise Ratio (WPSNR), Normalized cross-correlation (NC), and Structural Similarity Index (SSIM) than the conventional watermarking methods. This proposed method provides more robustness against several manipulations and lossy attacks.

© 2020 The Authors. Production and hosting by Elsevier B.V. on behalf of King Saud University. This is an open access article under the CC BY-NC-ND license (<http://creativecommons.org/licenses/by-nc-nd/4.0/>).

1. Introduction

The advanced development of internet technology leads to a massive transmission of digital media at a very high speed. In the meantime, technological development emerges outlaw manipulation of digital content. In this stance, digital watermarking is a boon to tackle this issue. This method embeds the secret information in a cover medium and this technique plays a significant role in protecting such digital media. Digital watermarking embedded in digital media like videos, images, audios and texts ensures the security of the digital information. Color image watermarking technique is utilized to conceal the data content (watermark) into the cover medium. Most of the existing watermark techniques use binary watermark as the embedding data, but according to the

recent development of media, professionals use the color watermark to secure their data. The effectiveness of the watermarking algorithm is assessed using imperceptible (invisible) and robustness (embedded watermark information cannot be easily removed by unauthorized users using cropping, filtering, rotation, etc.). Several researchers suggested various color image watermarking techniques (Singh, 2017; Su and Chen, 2018; Xiang-yang et al., 2012). Many watermarking techniques are used to achieve robust watermark (Bhatnagar et al., 2012; Yen and Huang, 2016). The domains used in watermarking techniques are spatial domain and frequency domain.

Spatial domain watermarking is a technique, (Araghi et al., 2016; Parashar and Singh, 2014) where the watermark embedding process is performed in the pixels of the host by altering a few pixel values. Methods commonly used in the spatial domain are histogram shifting, difference expansion and prediction error expansion (Chung et al., 2010; Horng et al., 2014). The histogram shifting (Ni et al., 2006) technique is used to embed the data on poles and carrier space. Besides, it provides a low embedding capacity. In difference expansion (Tian, 2003) technique, the difference between the set of adjacent pixels is computed and the one bit data is embedded into each set. This technique affords a high embedding capacity. Prediction error (Fallahpour, 2008) expansion technique estimates the error value from the host image and

* Corresponding author.

E-mail addresses: k.prabhajaya@gmail.com (K. Prabha), shatheeshsam@yahoo.com (I. Shatheesh Sam).

Peer review under responsibility of King Saud University.



Production and hosting by Elsevier

<https://doi.org/10.1016/j.jksuci.2020.04.003>1319-1578/© 2020 The Authors. Production and hosting by Elsevier B.V. on behalf of King Saud University. This is an open access article under the CC BY-NC-ND license (<http://creativecommons.org/licenses/by-nc-nd/4.0/>).

Please cite this article as: K. Prabha and I. Shatheesh Sam, An effective robust and imperceptible blind color image watermarking using WHT, Journal of King Saud University – Computer and Information Sciences, <https://doi.org/10.1016/j.jksuci.2020.04.003>

predicted image. The data embedding process is carried out on the error value and this technique offers lower distortion to the host image.

The transform domain is much more effective than the spatial domain by offering strong robustness against attacks. Rather than directly embedding data into the pixels, the frequency domain technique (Ganic and Eskicioglu, 2004) initially applies a transformation to convert the host image into the frequency domain; data embedding is done in the transformation coefficients. Some of the frequently used transformation techniques are the Discrete Fourier Transform (DFT), Discrete Cosine Transform (DCT) and Discrete Wavelet Transform (DWT) (Mehto and Mehra, 2016). Moreover, Singular Value Decomposition (SVD), QR (orthogonal-triangular) factorization and LU (lower-upper) decomposition are additionally utilized with these transformation methods.

The false positive problem is the major issue of SVD based watermarking. Guo and Prasetyo (2014) suggested a procedure to overcome this problem; initially, the host image is processed with DWT and SVD. The ambiguity situation and false positive issue are handled by embedding the primary component of a watermark into the host by modifying the largest singular value. Ansari and Pant (2017) depicted a hybrid watermarking scheme of DWT, SVD and Artificial Bee Colony (ABC). The host is preprocessed with DWT and SVD and the principal element of a watermark is embedded into the modified singular values. This method of embedding is one of the solutions for the false positive problem of SVD. Furthermore, ABC is utilized to improve the embedding strength of watermark to achieve maximum robustness.

Kalra et al. (2015) projected a blind color image watermarking algorithm using block based DCT. Double encryption technique, namely Arnold and Chaos are used to encrypt the watermark image. DWT is applied on the host after that middle frequency band undergoes 8×8 DCT transformation. In a 8×8 block of the DCT, nine frequencies in the middle are chosen for embedding watermark. For the watermark extraction process, inverse Arnold and inverse Chaos are performed. A hybrid robust color image watermarking scheme using Redundant Discrete Wavelet Transform (RDWT) and SVD (Roy and Pal, 2018) is proposed. The scrambled grayscale watermark image is inserted into the RDWT and SVD processed 8×8 non-overlapping blocks of the Y component of the host image. After embedding the watermark, Inverse RDWT is applied to each block. This scheme provides better effectiveness and imperceptibility.

An enhanced color image watermarking scheme (Su et al., 2019) is designed based on Schur decomposition. The RGB color watermark is transformed using Arnold transform and then it is converted to binary. The RGB host image is divided into 4×4 non-overlapping image blocks and the embedding blocks are chosen randomly using the MD 5 (Message Digest 5) algorithm. The watermark embedding procedure involves two methods. The first method is to embed the watermark in the unitary matrix of Schur decomposition and the second method is to embed the watermark in the upper triangular matrix of Schur decomposition. Embedding blocks are optimally chosen to embed watermark and the embedding flag is achieved. Through the embedding flag, the watermark image is extracted.

A blind color image watermarking scheme (Jia, 2014) is recommended using SVD. The RGB color host image is divided into 4×4 non-overlapping image block and SVD is applied on each block. By investigating the orthogonal matrix of SVD, it is clear that there is a strong correlation between the second row first column element and third row first column element. These elements are chosen for embedding the data as it exhibits a strong relationship. This relation is used to extract the data. This method resists common image manipulation attacks. Color image watermarking (Su et al.,

2012) is recommended using Schur decomposition. Data embedding is processed in the second row and third-row first column elements of the 4×4 unitary matrix because there exist a strong correlation. Data extraction is done using the relation between those elements. A blind color image watermarking using LU decomposition (Su et al., 2018) recommended without using any transform. Initially, the host image is subdivided into 4×4 matrix. The 4×4 matrix is then decomposed using LU decomposition. Arnold transform and MD 5 algorithm are used to increase watermark security and robustness. Here, the embedding process is done on two lower matrix coefficients since there exist similarity. In a 4×4 lower triangular matrix, one-bit data is embedded in the first column coefficients of the second row and third row. The embedding capacity of this method is 0.03125 bpp.

DFT and DCT are combined (Hamidi et al., 2018) to form a robust blind image watermarking technique. Such hybrid watermarking methods are utilized to achieve two important properties of watermarking, namely imperceptibility and robustness. Using QR decomposition a blind color image watermarking (Su et al., 2014a) scheme is proposed. The 4×4 non-overlapping blocks of the host are decomposed using QR decomposition. R matrix is chosen for watermark embedding. In order to preserve the quality of watermark, the first row fourth column coefficient of R matrix is quantified. Su et al. (2014b) suggested a blind watermarking scheme to reduce visual distortion using QR decomposition. The first column coefficients of the second-row and third-row in unitary matrix Q are selected for embedding watermark.

Liu et al. (2018) proposed an image watermarking scheme with a Laplacian Distribution based approach using wavelet subband, region texture and visual saliency characteristics. A visual saliency model is used to improve robustness. In view of achieving imperceptible watermarking, the image subblocks with high energy are chosen to embed the watermark information. The embedding capacity of the watermark is increased by selecting the region with rich texture besides this texture region tolerates more distortion. The watermark detection process includes the Laplacian distribution model to detect the watermark embedded subblock. By analyzing the previous works of literature, it is clear that several researchers focus mainly on less visual distortion and strong robustness. In this paper, the proposed method presents an effective blind color image watermarking using the Walsh Hadamard Transform (WHT). The main advantage of WHT is the fastest computation of WHT coefficients. The essential goal of the proposed method is to achieve image quality and effectiveness.

The contribution of this paper is structured as follows. Section 2 delineates the Walsh Hadamard Transform. Section 3 depicts the proposed blind color image watermarking. Section 4 discusses the experimental results of the proposed watermarking method and Section 5 concludes the proposed work.

2. Preliminary

2.1. Walsh Hadamard Transform

Walsh Hadamard Transform (WHT) (Meenakshi et al., 2014) is also known as Hadamard Transform or Walsh Transform or Walsh-Fourier Transform. WHT comes under the category of generalized Fourier transform. The benefit of using WHT is low computational complexity. It is an orthogonal function and consists of -1 and $+1$ values only. Walsh Transform is prominently suitable for various applications such as image processing, speech processing, filtering, and power spectrum analysis ("Walsh-Hadamard Transform – MATLAB & Simulink – MathWorks India," n.d.). The Walsh Hadamard Transform for a sequence $f(x)$ having 'N' number of samples is represented as,

$$F(U) = \frac{1}{N} \times [H_N] \times f(x) \quad (1)$$

where, $F(U)$ is the Walsh Hadamard Transform of $f(x)$ and $[H_N]$ is the Hadamard square matrix and its size is $N \times N$.

The 2×2 Hadamard square matrix is written as,

$$[H_2] = \begin{bmatrix} 1 & 1 \\ 1 & -1 \end{bmatrix} \quad (2)$$

The 4×4 Hadamard square matrix is written as,

$$[H_4] = \begin{bmatrix} H_2 & H_2 \\ H_2 & -H_2 \end{bmatrix} = \begin{bmatrix} 1 & 1 & 1 & 1 \\ 1 & -1 & 1 & -1 \\ 1 & 1 & -1 & -1 \\ 1 & -1 & -1 & 1 \end{bmatrix} \quad (3)$$

Therefore, the general form of the Walsh Hadamard Transform is,

$$[H_{2^p}] = \begin{bmatrix} H_{2^{p-1}} & H_{2^{p-1}} \\ H_{2^{p-1}} & -H_{2^{p-1}} \end{bmatrix} \text{ for } p = 1, 2, 3 \dots \quad (4)$$

where, the p value depends on the value of N , i.e. $N = 2^p$.

The inverse WHT of a 1 Dimensional sequence is denoted as,

$$f(x) = [H_N] \times F(U) \quad (5)$$

Like the above Equations, the Walsh Hadamard Transform of a 2 Dimensional image $f(x,y)$ is represented as,

$$F(U,V) = \frac{1}{N} \times [H_N] \times f(x,y) \quad (6)$$

where, $F(U,V)$ is the WHT of $f(x,y)$.

The inverse 2 Dimensional WHT is given as,

$$f(x,y) = [H_N] \times F(U,V) \quad (7)$$

The below example explains the forward and inverse 2-D Walsh Hadamard Transform. Let us consider a 4×4 image block which is given by,

$$f(x,y) = \begin{bmatrix} 120 & 180 & 15 & 80 \\ 97 & 48 & 55 & 16 \\ 78 & 89 & 129 & 201 \\ 47 & 189 & 96 & 46 \end{bmatrix} \quad (8)$$

The 4×4 image block $f(x,y)$ is transformed using WHT and the WHT coefficients are computed as,

$$F(U,V) = \frac{1}{4} \times \begin{bmatrix} 1 & 1 & 1 & 1 \\ 1 & -1 & 1 & -1 \\ 1 & 1 & -1 & -1 \\ 1 & -1 & -1 & 1 \end{bmatrix} \times \begin{bmatrix} 120 & 180 & 15 & 80 \\ 97 & 48 & 55 & 16 \\ 78 & 89 & 129 & 201 \\ 47 & 189 & 96 & 46 \end{bmatrix} = \begin{bmatrix} 85.5 & 126.5 & 73.75 & 85.75 \\ 13.5 & 8 & -1.75 & 54.75 \\ 23 & -12.5 & -38.75 & -37.75 \\ -2 & 58 & -18.25 & -22.75 \end{bmatrix} \quad (9)$$

The inverse of 4×4 image block $F(U,V)$ is computed as,

$$f(x,y) = \begin{bmatrix} 1 & 1 & 1 & 1 \\ 1 & -1 & 1 & -1 \\ 1 & 1 & -1 & -1 \\ 1 & -1 & -1 & 1 \end{bmatrix} \times \begin{bmatrix} 85.5 & 126.5 & 73.75 & 85.75 \\ 13.5 & 8 & -1.75 & 54.75 \\ 23 & -12.5 & -38.75 & -37.75 \\ -2 & 58 & -18.25 & -22.75 \end{bmatrix} = \begin{bmatrix} 120 & 180 & 15 & 80 \\ 97 & 48 & 55 & 16 \\ 78 & 89 & 129 & 201 \\ 47 & 189 & 96 & 46 \end{bmatrix} \quad (10)$$

The general form of WHT for the 4×4 image block $f(x,y)$ is denoted as,

$$F(U,V) = \begin{bmatrix} a_{11} & a_{12} & a_{13} & a_{14} \\ a_{21} & a_{22} & a_{23} & a_{24} \\ a_{31} & a_{32} & a_{33} & a_{34} \\ a_{41} & a_{42} & a_{43} & a_{44} \end{bmatrix} \quad (11)$$

The coefficient sets (a_{31}, a_{41}) , (a_{32}, a_{42}) , (a_{33}, a_{43}) and (a_{34}, a_{44}) are used to embed the 4-bit data in these coefficients sets as shown in Fig. 1. The third and fourth-row elements are chosen for embedding the data because a slight change in those elements does not excessively affect the quality of the image.

3. Proposed method

The important feature of the proposed method is that even a slight variation in the third and fourth row of the WHT coefficients may not profoundly affect the visual quality of the image. Thus, it influences the watermark embedding scheme to attain a better quality watermarked image and helps to achieve strong robustness against attack. In this section, the embedding and extraction process of the proposed blind color image watermark based on WHT are explained.

3.1. Watermark embedding

Fig. 2 illustrates the block diagram of the proposed watermark embedding process.

Let us consider $I(x,y,z)$ as the color host image and $D(x,y,z)$ as the color watermark image. The image $D(x,y,z)$ is embedded in $I(x,y,z)$ to get the watermarked image $W(x,y,z)$. Initially, the host cover image $I(x,y,z)$ is partitioned into 4×4 non-overlapping blocks. Each non-overlapping block is transformed by Walsh Hadamard Transform using Eq. (6). In a 4×4 block, the third and fourth-row consist of eight coefficients; hence, 4-bit is embedded in these sixteen coefficients. The 4-bit data is hidden into the third and fourth-row elements of the transformed coefficients as shown in Fig. 3.

In Fig. 3, a_{3i} is the third-row coefficient, where $a_{3i} = \{a_{31}, a_{32}, a_{33}, a_{34}\}$ and a_{4i} is the fourth-row coefficient, where $a_{4i} = \{a_{41}, a_{42}, a_{43}, a_{44}\}$. Let e_{3i} and e_{4i} be the data embedded third-row and fourth-row coefficients, where $e_{3i} = \{e_{31}, e_{32}, e_{33}, e_{34}\}$ and $e_{4i} = \{e_{41}, e_{42}, e_{43}, e_{44}\}$. The 4-bit data $b_i = \{b_1, b_2, b_3, b_4\}$ is embedded in the coefficients a_{3i} and a_{4i} to get the embedded coefficients e_{3i} and e_{4i} .

The steps for embedding data is as follows,

Step 1: From the coefficients a_{3i} and a_{4i} , estimate the difference d_i and average avg_i .

$$d_i = |a_{3i} - a_{4i}| \quad (12)$$

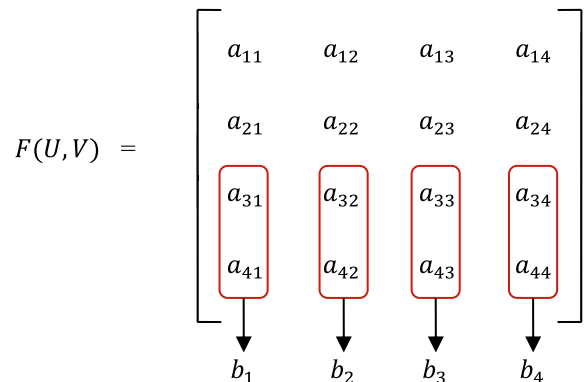


Fig. 1. Walsh Hadamard Transform.

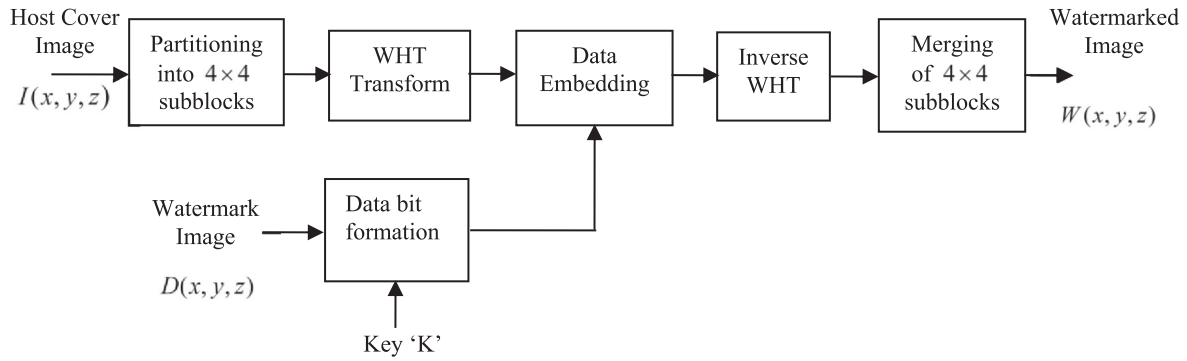


Fig. 2. Block diagram of the proposed data (watermark) embedding algorithm.

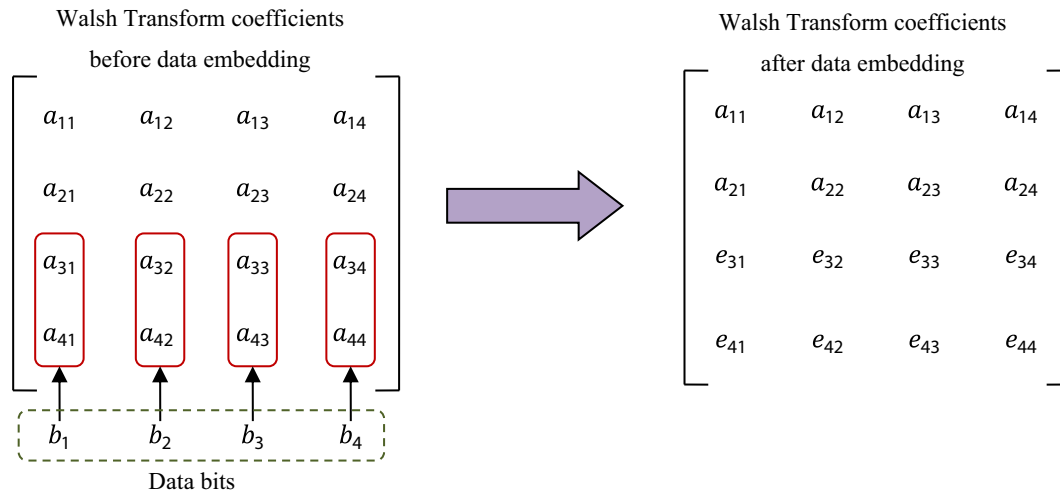


Fig. 3. Embedding of data on Walsh Hadamard coefficients.

$$avg_i = \frac{(\lfloor a_{3i} \rfloor + |a_{4i}|)}{2} \quad (13)$$

where, $\lfloor \cdot \rfloor$ is the floor function and $|\cdot|$ is the absolute function.

Step 2: Based on the difference d_i and binary data b_i calculate the data embedded coefficients l_i and m_i as,

If $rem(|d_i|, 2) = 0$

$$l_i = \begin{cases} avg_i - \left(\frac{d_i}{2}\right) & \text{if } b_i = 0 \\ avg_i - \left(\frac{d_i}{2} - 0.5\right) & \text{if } b_i = 1 \end{cases} \quad (14)$$

$$m_i = \begin{cases} avg_i + \left(\frac{d_i}{2}\right) & \text{if } b_i = 0 \\ avg_i + \left(\frac{d_i}{2} - 0.5\right) & \text{if } b_i = 1 \end{cases} \quad (15)$$

If $rem(|d_i|, 2) = 1$

$$l_i = \begin{cases} avg_i - \left(\frac{d_i}{2}\right) & \text{if } b_i = 1 \\ avg_i - \left(\frac{d_i}{2} - 0.5\right) & \text{if } b_i = 0 \end{cases} \quad (16)$$

$$m_i = \begin{cases} avg_i + \left(\frac{d_i}{2}\right) & \text{if } b_i = 1 \\ avg_i + \left(\frac{d_i}{2} - 0.5\right) & \text{if } b_i = 0 \end{cases} \quad (17)$$

where, $rem(|d_i|, 2)$ is the remainder obtained while dividing $|d_i|$ by 2.

Step 3: Replace the values of l_i and m_i in the place of a_{3i} and a_{4i} depending on the minimum and maximum values to get the embedded coefficients e_{3i} and e_{4i} .

$$e_{3i} = \begin{cases} \max(l_i, m_i) & \text{if } a_{3i} \geq a_{4i} \\ \min(l_i, m_i) & \text{if } a_{3i} < a_{4i} \end{cases} \quad (18)$$

$$e_{4i} = \begin{cases} \max(l_i, m_i) & \text{if } a_{4i} \geq a_{3i} \\ \min(l_i, m_i) & \text{if } a_{4i} < a_{3i} \end{cases} \quad (19)$$

After embedding the data, the Walsh Hadamard embedded coefficients are represented as,

$$F(U, V) = \begin{bmatrix} a_{11} & a_{12} & a_{13} & a_{14} \\ a_{21} & a_{22} & a_{23} & a_{24} \\ e_{31} & e_{32} & e_{33} & e_{34} \\ e_{41} & e_{42} & e_{43} & e_{44} \end{bmatrix} \quad (20)$$

After attaining the Walsh Hadamard embedded coefficients, calculate the inverse Walsh Hadamard Transform of each 4×4 subblock. Merge all the 4×4 subblocks to get the watermarked image $W(x, y, z)$. Based on the above steps, the watermark is embedded on the host image as shown in Fig. 2.

Algorithm 1: Data Embedding using WHT

Input: Host Cover Image, Watermark Image

Step 1: Convert the watermark image pixels $D(x, y, z)$ to binary data b_i after shuffling using the key 'K'.

Step 2: Partition the host cover image $I(x, y, z)$ into 4×4 non-overlapping blocks.

Step 3: Obtain the WHT transform of each block using Equation (6).

Step 4: Obtain the difference and average value of the third and fourth row WHT coefficients as discussed in Eqs. (12) and (13).

Step 5: Based on the value of $\text{rem}(|d_i|, 2)$ and binary data b_i , obtain the value of l_i and m_i using Eqs. (14)–(17).

Step 6: Estimate the values of e_{3i} and e_{4i} using the minimum and maximum values of a_{3i} , a_{4i} and l_i and m_i using Eqs. (18) and (19). Using the value of e_{3i} and e_{4i} , form the WHT embedded coefficient matrix as shown in Eq. (20).

Step 7: Find the floor value of the inverse WHT values of each 4×4 WHT embedded coefficients.

Step 8: Merge all the 4×4 subblocks obtained in step 7 to get the watermarked image $W(x, y, z)$.

Output: Watermarked Image

The proposed data embedding algorithm is explained below with an example. Consider a 4×4 subblock of a host image given by,

$$I(x, y) = \begin{bmatrix} 120 & 180 & 15 & 80 \\ 97 & 48 & 55 & 16 \\ 78 & 89 & 129 & 201 \\ 47 & 189 & 96 & 46 \end{bmatrix} \quad (21)$$

The WHT 4×4 coefficients of $I(x, y)$ is given by,

$$I(U, V) = \begin{bmatrix} 85.5 & 126.5 & 73.75 & 85.75 \\ 13.5 & 8 & -1.75 & 54.75 \\ 23 & -12.5 & -38.75 & -37.75 \\ -2 & 58 & -18.25 & -22.75 \end{bmatrix} \quad (22)$$

Here, the third-row coefficient is $a_{3i} = \{23, -12.5, -38.75, -37.75\}$ and fourth-row coefficient is $a_{4i} = \{-2, 58, -18.25, -22.75\}$. Let $b_i = \{1, 0, 1, 0\}$ be the data to embed. The difference and average value of the third and fourth-row WHT coefficients using Eqs (12) and (13) is given as $d_i = \{25, 70, 20, 15\}$ and $\text{avg}_i = \{10.5, 23, -28, -29.5\}$. From the difference d_i and avg_i , the value of l_i and m_i is calculated using Eqs. (14)–(17) as $l_i = \{-2, -12, -37.5, -36.5\}$ and $m_i = \{23, 58, -18.5, -22.5\}$. Using the minimum and maximum values of l_i , m_i and a_{3i} , a_{4i} , the data embedded WHT coefficients are $e_{3i} = \{23, -12, -37.5, -36.5\}$ and $e_{4i} = \{-2, 58, -18.5, -22.5\}$.

The embedded coefficients are written as,

$$W(U, V) = \begin{bmatrix} 85.5 & 126.5 & 73.75 & 85.75 \\ 13.5 & 8 & -1.75 & 54.75 \\ 23 & -12 & -37.5 & -36.5 \\ -2 & 58 & -18.5 & -22.5 \end{bmatrix} \quad (23)$$

The Inverse WHT of the coefficients $W(U, V)$ is

$$W(x, y) = \begin{bmatrix} 120 & 180 & 16 & 81 \\ 97 & 48 & 56 & 17 \\ 78 & 88 & 128 & 199 \\ 47 & 188 & 94 & 45 \end{bmatrix} \quad (24)$$

3.2. Watermark extraction

Fig. 4 illustrates the watermark extraction process, which is the inverse of the watermark embedding process.

The watermarked image $W(x, y, z)$ is partitioned into 4×4 non-overlapping subblocks in which each subblock is converted to WHT coefficients using WHT transform as shown in Eq. (6). The data is extracted from the third and fourth-row WHT coefficients using Eqs. (26) and (27).

Let the data embedded WHT coefficients are written by,

$$W(U, V) = \begin{bmatrix} \hat{a}_{11} & \hat{a}_{12} & \hat{a}_{13} & \hat{a}_{14} \\ \hat{a}_{21} & \hat{a}_{22} & \hat{a}_{23} & \hat{a}_{24} \\ \hat{e}_{31} & \hat{e}_{32} & \hat{e}_{33} & \hat{e}_{34} \\ \hat{e}_{41} & \hat{e}_{42} & \hat{e}_{43} & \hat{e}_{44} \end{bmatrix} \quad (25)$$

The difference \hat{d}_i between the values \hat{e}_{3i} and \hat{e}_{4i} is calculated using,

$$\hat{d}_i = |\hat{e}_{3i} - \hat{e}_{4i}| \quad (26)$$

where, \hat{e}_{3i} and \hat{e}_{4i} is the third-row and fourth-row data embedded WHT coefficient.

The hidden data \hat{b}_i is extracted from the value \hat{d}_i as,

$$\hat{b}_i = \text{rem}(\lfloor \hat{d}_i \rfloor, 2) \quad (27)$$

Algorithm 2: Data extraction based on WHT

Input: Watermarked Image

Step 1: Partition the watermarked image $W(x, y, z)$ into 4×4 non-overlapping blocks.

Step 2: Obtain the WHT of each subblock.

Step 3: From the coefficients \hat{e}_{3i} and \hat{e}_{4i} , find the difference \hat{d}_i using Eq. (26).

Step 4: Extract the data \hat{b}_i using Eq. (27).

Step 5: From the extracted data \hat{b}_i reconstruct the watermark image using the key 'K' by rearranging the pixel values.

Output: Extracted Watermark

The proposed data extraction method is explained with an example. Consider a 4×4 subblock of the watermarked image.

$$W(x, y) = \begin{bmatrix} 120 & 180 & 16 & 81 \\ 97 & 48 & 56 & 17 \\ 78 & 88 & 128 & 199 \\ 47 & 188 & 94 & 45 \end{bmatrix} \quad (28)$$

The WHT transform of $W(x, y)$ is given by,

$$W(U, V) = \begin{bmatrix} 85.5 & 126.5 & 73.75 & 85.75 \\ 13.5 & 8 & -1.75 & 54.75 \\ 23 & -12 & -37.5 & -36.5 \\ -2 & 58 & -18.5 & -22.5 \end{bmatrix} \quad (29)$$

The third-row watermark embedded coefficients are $\hat{e}_{3i} = \{23, -12, -37.5, -36.5\}$ and the watermark embedded fourth-row coefficients are $\hat{e}_{4i} = \{-2, 58, -18.5, -22.5\}$. From the

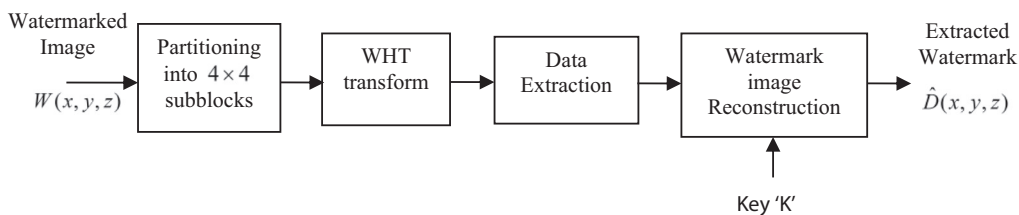


Fig. 4. Block diagram of the proposed data (watermark) extraction algorithm.

value of \hat{e}_{3i} and \hat{e}_{4i} , the difference \hat{d}_i is estimated using Eq. (26) as $\hat{d}_i = \{25, 70, 19, 14\}$. From the value of \hat{d}_i , the data $\hat{b}_i = \{1, 0, 1, 0\}$ is extracted using Eq. (27). Thus the watermark information is blindly extracted from the host image.

4. Experimental results

The proposed WHT based watermarking algorithm is tested for imperceptibility and robustness. The proposed algorithm is analyzed and evaluated by embedding capacity, visual quality (PSNR and WPSNR), Structural Similarity Index (SSIM) and Normalized cross-correlation (NC). The NC metric is used to evaluate the watermark robustness; whereas the PSNR, WPSNR and SSIM metrics are used to measure the image quality. The experimental analysis is implemented using MATLAB R2015a.

The performance is verified using seven test images, as shown in Fig. 5. The 24-bit RGB images of dimension 512×512 are used as host cover images which are chosen from CVG-UGR ("CVG – UGR – Image database," n.d.) and USC-SIPI ("SIPI Image Database – Misc," n.d.) image database. The three 24-bit RGB images of dimension 90×90 are used as the watermark logo images. The executions are performed with MATLAB R2015a, Intel Core i7, CPU @ 2.60 GHz, 8 GB RAM, Windows 10.

The image fidelity metrics such as PSNR, WPSNR and SSIM are used to assess the quality of the image. Let us consider $I(x, y, z)$ as the RGB host image and $W(x, y, z)$ as the watermark embedded image of size $M \times N$. The below relation is used to estimate the PSNR value.

$$PSNR = 10 \times \log_{10} \left(\frac{(\max(I(x, y, z))^2)}{MSE} \right) \quad (30)$$

The Mean Square Error (MSE) is calculated using the following relation,

$$MSE = \frac{1}{3 \times M \times N} \sum_{z=1}^3 \sum_{x=1}^M \sum_{y=1}^N [W(x, y, z) - I(x, y, z)]^2 \quad (31)$$

Another important perceptual quality metric is Weighted PSNR. WPSNR is used to calculate the weighted peak signal to noise ratio between the RGB host image $I(x, y, z)$ and the watermark embed-

ded image $W(x, y, z)$. WPSNR introduces an additional parameter named noise visibility function (NVF). NVF is a texture masking function which acts as the penalization factor.

The WPSNR is calculated using the following relations,

$$WPSNR = 20 \log_{10} \left(\frac{(\max(I(x, y, z)))}{\sqrt{WMSE}} \right) \quad (32)$$

$$WMSE = \frac{1}{3 \times M \times N} \sum_{z=1}^3 \sum_{x=1}^M \sum_{y=1}^N NVF \times (I(x, y, z) - W(x, y, z))^2 \quad (33)$$

$$NVF = \frac{1}{1 + \theta \sigma_I^2(x, y, z)} \quad (34)$$

where, θ represents the tuning parameter of the particular image and σ_I^2 represents the local variance of the specific image with 3×3 window.

The Structural Similarity Index (SSIM) is the metric to predict the visual quality of the image. The SSIM value is computed using the below relation,

$$SSIM = L(W, I)C(W, I)S(W, I) \quad (35)$$

where, $L(W, I)$ represents luminance comparison, $C(W, I)$ represents contrast comparison and $S(W, I)$ represents saturation comparison.

The watermark robustness is measured by Normalized cross-correlation (NC). Normalized cross-correlation specifies the correlation between the original watermark image $D(x, y, z)$ and the extracted watermark image $\hat{D}(x, y, z)$ which is calculated using the relation,

$$NC = \frac{\sum_{z=1}^3 \sum_{x=1}^p \sum_{y=1}^q D(x, y, z) \times \hat{D}(x, y, z)}{\sqrt{\sum_{z=1}^3 \sum_{x=1}^p \sum_{y=1}^q D(x, y, z)^2} \sqrt{\sum_{z=1}^3 \sum_{x=1}^p \sum_{y=1}^q \hat{D}(x, y, z)^2}} \quad (36)$$

where, $p \times q$ indicates the dimension of the watermark image.

Table 1 depicts the PSNR, WPSNR, SSIM and NC values for an embedding capacity of 0.25 bpp. The PSNR of the proposed system is greater than 49 dB for all the test images, whereas the WPSNR value is around 49 dB and SSIM value is higher than 0.9925. The PSNR and WPSNR are approximately equal to each other. It is understandable from Table 1 that the NC value is best for the test

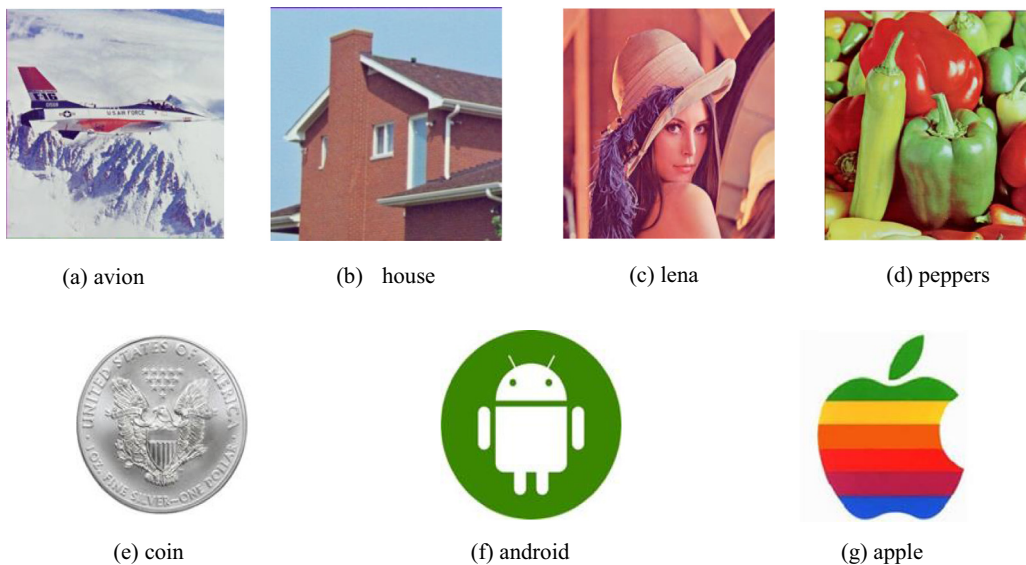


Fig. 5. Test images, (a)–(d) Host cover images (e)–(g) Watermark logo images.

Table 1

PSNR, WPSNR, SSIM and NC comparison of the proposed watermarking methods.

Cover Image	Coin				Android				Apple			
	PSNR (dB)	WPSNR (dB)	SSIM	NC	PSNR (dB)	WPSNR (dB)	SSIM	NC	PSNR (dB)	WPSNR (dB)	SSIM	NC
Avion	49.2355	49.2666	0.9941	1	49.2360	49.2656	0.9941	1	49.2336	49.2639	0.9941	1
House	49.3922	49.6025	0.9931	1	49.4321	49.6501	0.9932	1	49.3814	49.5908	0.9931	1
Lena	49.2075	49.8871	0.9948	1	49.2055	49.8839	0.9948	1	49.1996	49.8784	0.9948	1
Peppers	49.2645	49.6554	0.9952	0.9999	49.2705	49.6625	0.9951	0.9998	49.2633	49.6566	0.9952	0.9999

Table 2

PSNR, SSIM and NC of the proposed watermarking method for different cover images and watermark image 'coin'.

bpp	Avion			House			Lena			Peppers		
	PSNR (dB)	SSIM	NC	PSNR (dB)	SSIM	NC	PSNR (dB)	SSIM	NC	PSNR (dB)	SSIM	NC
0.25	49.2355	0.9941	1	49.3922	0.9931	1	49.2075	0.9948	1	49.2645	0.9952	0.9999
0.21875	49.8369	0.9943	1	50.0426	0.9934	1	49.8118	0.9950	1	49.8462	0.9953	0.9999
0.1875	50.4872	0.9945	1	50.6771	0.9936	1	50.4738	0.9952	1	50.4895	0.9955	1.0000
0.15625	51.3002	0.9952	1	51.4662	0.9944	1	51.2880	0.9958	1	51.2822	0.9960	0.9999
0.125	52.1903	0.9961	1	52.3812	0.9958	1	52.1877	0.9967	1	52.1416	0.9970	0.9999
0.09375	53.5091	0.9978	0.9999	53.6986	0.9980	0.9999	53.5438	0.9980	0.9999	53.4192	0.9982	0.9999
0.0625	55.2712	0.9987	0.9999	55.4737	0.9991	0.9999	55.2815	0.9988	0.9999	55.1527	0.9989	0.9999
0.03125	58.2298	0.9991	0.9998	58.5624	0.9995	0.9998	58.2618	0.9993	0.9998	58.1286	0.9994	0.9998

Table 3

PSNR and WPSNR comparison of the proposed watermarking method for different embedding capacities with 'coin' as watermark image.

bpp	Avion		House		Lena		Peppers	
	PSNR (dB)	WPSNR (dB)	PSNR (dB)	WPSNR (dB)	PSNR (dB)	WPSNR (dB)	PSNR (dB)	WPSNR (dB)
0.25	49.2355	49.2666	49.3922	49.6025	49.2075	49.8871	49.2645	49.6554
0.21875	49.8369	49.9486	50.0426	50.3806	49.8118	50.6028	49.8462	50.4024
0.1875	50.4872	51.1941	50.6771	51.6937	50.4738	51.9030	50.4895	51.7302

Table 4

The watermark embedding capacity comparison of various watermarking methods.

Methods	Watermark length (bit)	Host image (pixel)	Bit/Pixel
SVD based data hiding	$32 \times 32 \times 24$	$512 \times 512 \times 3$	0.03125
Schur decomposition based data hiding	$32 \times 32 \times 24$	$512 \times 512 \times 3$	0.03125
LU decomposition based data hiding	$32 \times 32 \times 24$	$512 \times 512 \times 3$	0.03125
Laplacian Distribution based data hiding	$32 \times 32 \times 24$	$512 \times 512 \times 3$	0.03125
Proposed Method	$90 \times 90 \times 24$	$512 \times 512 \times 3$	0.25

images avion, house and lena is '1' while it is 0.999 for the test image peppers.

Table 2 depicts the performance of the proposed watermarking method in terms of PSNR, SSIM and NC for different embedding capacity with coin image as watermark. The PSNR is around 49 dB for an embedding capacity of 0.25 bpp. The PSNR value

increases as embedding capacity decrease. The PSNR is about 58 dB for an embedding capacity of 0.03125 bpp. The high PSNR value depicts that the proposed scheme is highly imperceptible and the distortion of the watermark image is very less. The SSIM is around 0.994 for an embedding capacity of 0.25 bpp and 0.999 for an embedding capacity of 0.03125 bpp. The NC values for the varying embedding capacities are very close to 1.

The PSNR and WPSNR values for different embedding capacities are tabulated in Table 3. For the embedding capacities 0.25 and 0.21875, the PSNR and WPSNR are approximately equal for all the test images. But for the embedding capacity of 0.1875, there is a little variation in the PSNR and WPSNR.

The embedding capacity is calculated as,

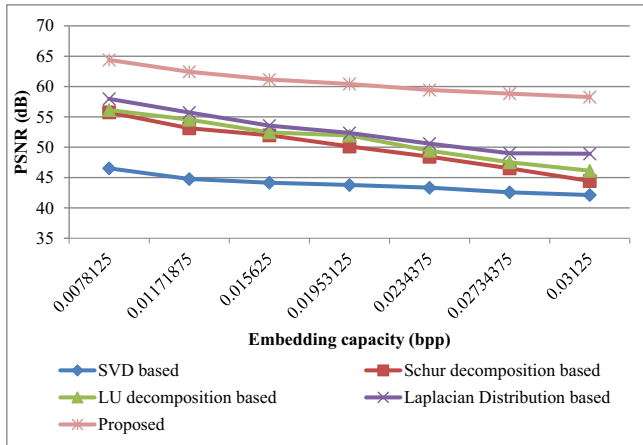
$$(90 \times 90 \times 24) / (512 \times 512 \times 3) = 0.25 \text{bpp}$$

The embedding capacity of different conventional watermarking methods is compared with the proposed watermarking methods are tabulated in Table 4. The proposed watermarking method provides an outstanding embedding capacity of 0.25 bpp.

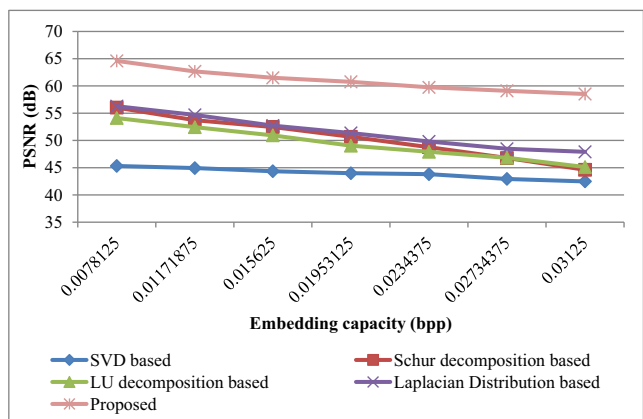
Table 5

PSNR and SSIM comparison of various watermarking methods on cover image 'lena' and watermark image 'apple'.

bpp	SVD based		Schur decomposition based		LU decomposition based		Laplacian Distribution based		Proposed	
	PSNR (dB)	SSIM	PSNR (dB)	SSIM	PSNR (dB)	SSIM	PSNR (dB)	SSIM	PSNR (dB)	SSIM
0.03125	42.122	0.954	44.437	0.962	46.124	0.971	48.922	0.980	58.2590	0.9993
0.02734375	42.561	0.958	46.520	0.968	47.525	0.975	49.007	0.982	58.8339	0.9994
0.0234375	43.333	0.962	48.431	0.971	49.432	0.977	50.591	0.984	59.4256	0.9995
0.01953125	43.777	0.965	50.124	0.977	51.931	0.981	52.356	0.988	60.4285	0.9996
0.015625	44.154	0.971	51.963	0.981	52.450	0.983	53.562	0.990	61.1548	0.9996
0.01171875	44.761	0.978	53.128	0.983	54.538	0.985	55.724	0.992	62.4382	0.9997
0.0078125	46.520	0.982	55.752	0.986	56.123	0.989	57.970	0.994	64.3830	0.9998



(a)

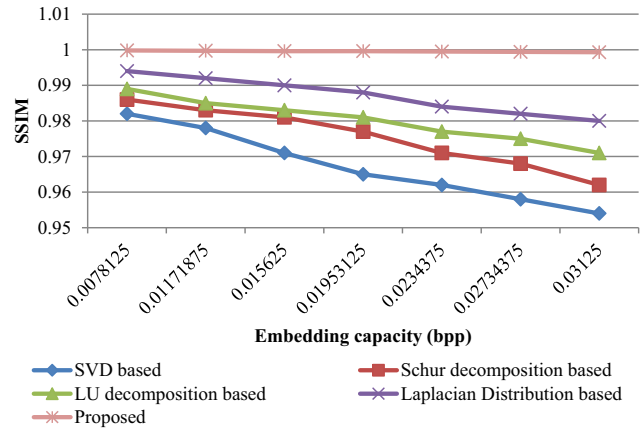


(b)

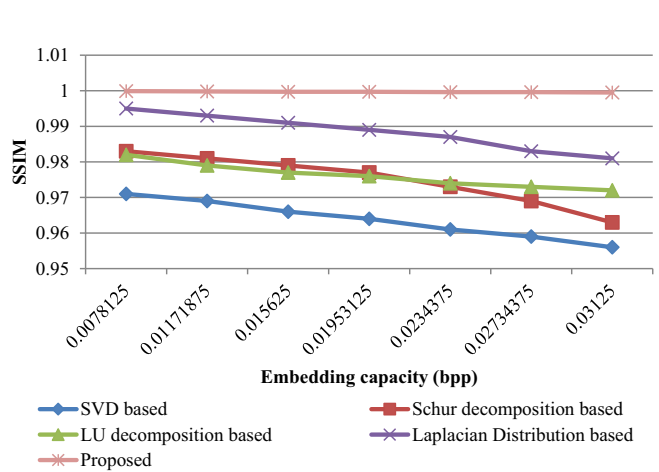
Fig. 6. PSNR comparison of the proposed system and conventional schemes (a) host image 'lena' and watermark image 'apple' (b) host image 'house' and watermark image 'apple'.

Table 5 shows the PSNR and SSIM comparison of different watermarking methods with the proposed watermarking method. The proposed method shows a very high PSNR over the conventional techniques such as SVD based data hiding (Jia, 2014), Schur decomposition based data hiding (Su et al., 2012), LU decomposition based data hiding (Su et al., 2018) and Laplacian Distribution based data hiding (Liu et al., 2018). For an embedding capacity of 0.03125 bpp, the proposed data hiding method provides a PSNR of 58 dB, while the conventional method provides PSNR less than 49 dB.

From Table 5, the minimum PSNR value attained for the conventional watermarking method is 42.122 dB, whereas the minimum PSNR value achieved for the proposed watermarking



(a)



(b)

Fig. 7. SSIM comparison of the proposed system and conventional schemes (a) host image 'lena' and watermark image 'apple' (b) host image 'house' and watermark image 'apple'.

method is 58.2590 dB. The optimum PSNR value obtained for the traditional watermarking method is 57.970 dB, whereas the optimum PSNR value of the proposed watermarking method is 64.3830 dB. Extremely high PSNR value is achieved using this proposed method.

Fig. 6 illustrates the performance comparison of the proposed system and conventional watermarking methods for different embedding capacity. While comparing the proposed data hiding approach with the traditional data hiding approaches, it is clear that the proposed method provides a high PSNR for different embedding capacities.

Table 6
Some of the different types of attacks for robustness measurement.

Salt and Pepper noise	Mean '0.01'	Mean '0.02'	Mean '0.03'	Mean '0.04'
Median filtering	Mask size 3×1	Mask size 5×1	Mask size 7×1	Mask size 9×1
Cropping	25% Cropping	40% Cropping	50% Cropping	60% Cropping
JPEG 2000	Compression Ratio 2:1	Compression Ratio 3:1	Compression Ratio 4:1	Compression Ratio 5:1
Compression				
Rotation	10°	20°	30°	40°
Brighten	Adding 10 to each pixels	Adding 30 to each pixels	Adding 60 to each pixels	Adding 90 to each pixels
Darken	Subtracting 20 from each pixels	Subtracting 40 from each pixels	Subtracting 60 from each pixels	Subtracting 80 from each pixels
Combinatorial Attacks	Scaling(1.5) + Rotation(10°)	Scaling(1.5) + Gamma Correction	Motion Blur + Contrast Adjustment	Sharpening(0.2) + Contrast Adjustment

Fig. 7 shows the graph between NC and embedding capacity. In the proposed method, the NC value is almost unity for different embedding capacity and for the conventional data hiding approaches it decreases as the embedding capacity increases. The NC value around unity in proposed method resembles that the hidden watermark image and extracted watermark image are almost similar.

To check the robustness of the proposed watermarking algorithm, the watermarked image is exposed to different attacks such

as scaling, rotation, contrast adjustment, gamma correction, Gaussian low pass filter, butterworth high pass, brighten, darken, scaling and rotation, salt and pepper noise, median filtering, cropping and JPEG 2000 compression. The watermark image is subjected to different attacks of different intensity which is shown in Table 6.

The proposed watermarking algorithm is tested on different manipulation and combinatorial attacks as presented in Fig. 8. Fig. 8 depicts the robustness of the proposed watermarking algo-

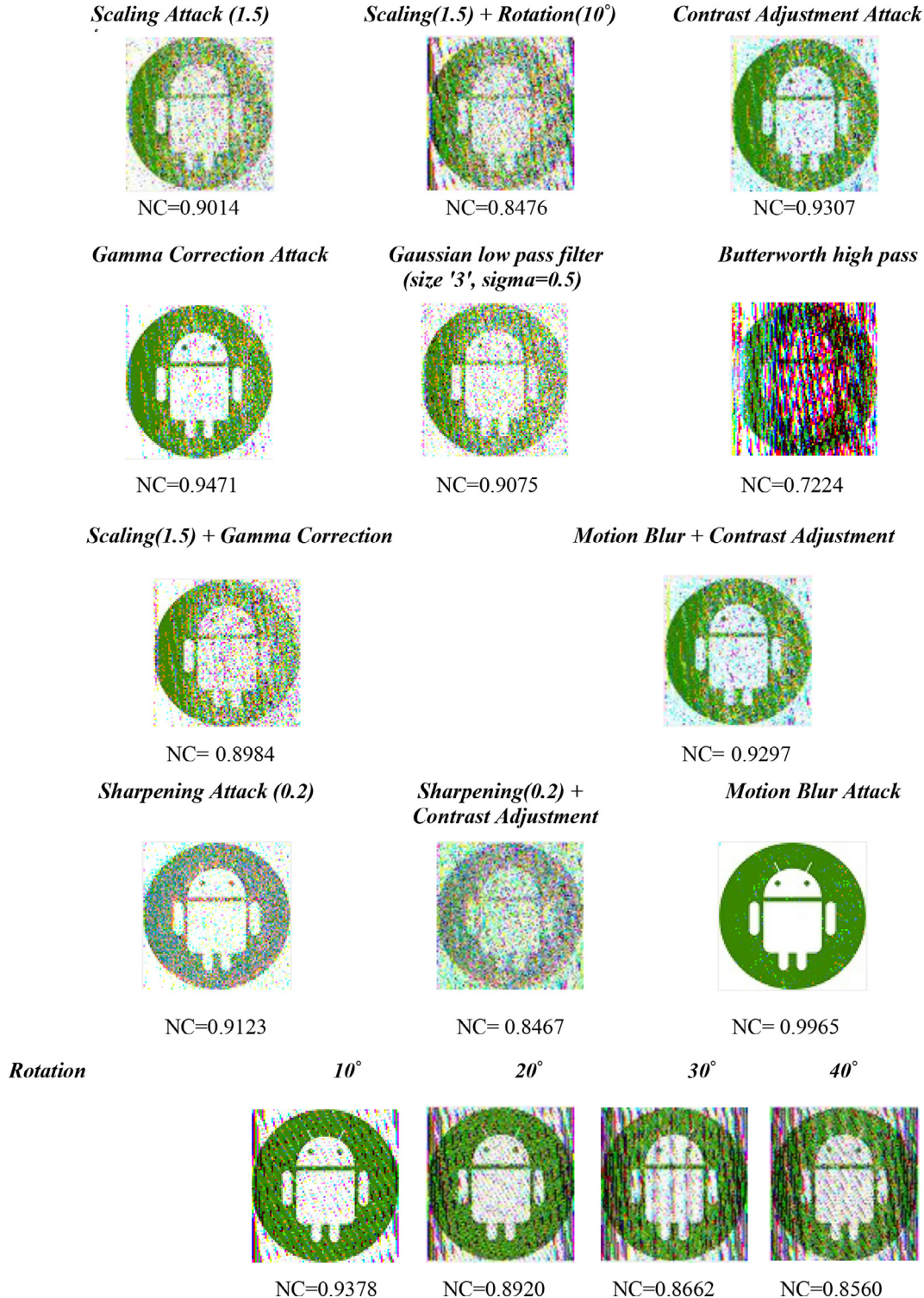


Fig. 8. Comparison of extracted watermarks from the watermarked image with various attacks (host image 'house' and watermark image 'android').

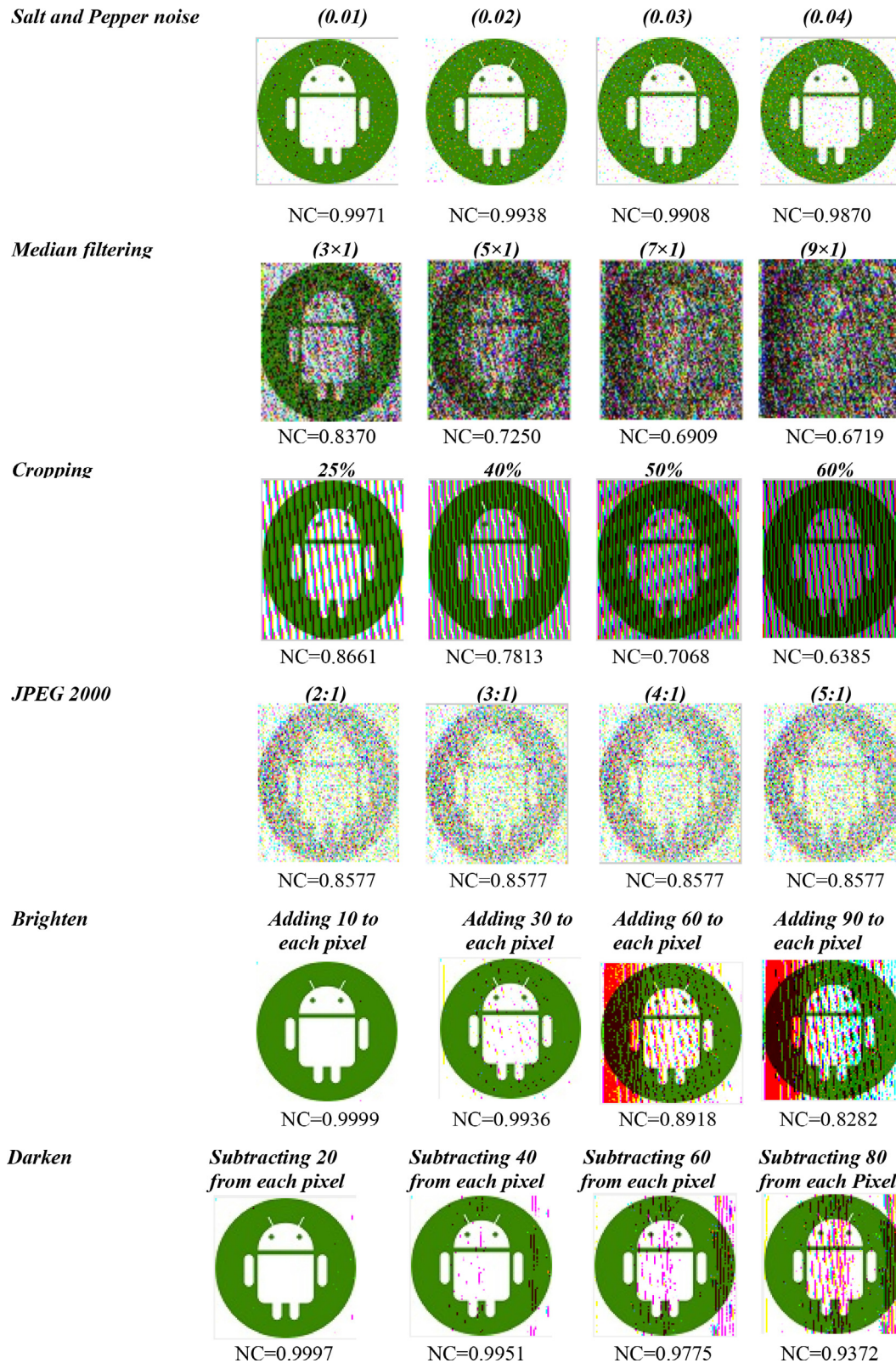


Fig. 8 (continued)

rithm for the host image 'house' and watermark image 'android'. The proposed watermarking algorithm is highly resistant to different attacks as shown in Fig. 8.

The reliability of the proposed method is guaranteed by testing it with different manipulation attacks and some combinatorial

attacks. The proposed watermarking algorithm offers high NC for the attacks such as Motion blur, sharpening, scaling, contrast adjustment, gamma correction, Gaussian low pass filter, Rotation 10°, brighten (adding 10 & 30 to each pixel), salt and pepper noise for the noise densities 0.01, 0.02, 0.03 and 0.04, median filtering

Table 7

Computational complexity comparison of the proposed method with other existing methods.

Methods	Embedding Time (s)	Extraction Time (s)	Overall Computational Complexity (s)
SVD based data hiding	1.2907	0.4891	1.7798
Schur decomposition based data hiding	1.2363	0.4917	1.728
LU decomposition based data hiding	0.8026	0.2162	1.0188
Laplacian Distribution based data hiding	1.1836	0.3520	1.5356
Proposed Method	0.7901	0.2015	0.9916

(3 × 1) and 25% cropping, whereas the NC is low for brightening (adding 90 to each pixel), median filtering (9 × 1) and 60% cropping. Moreover, for the darken attack, the NC value is close to 1. In the case of JPEG-2000 compression, the NC is almost constant for different compression ratio such as 2:1, 3:1, 4:1 and 5:1. Some combinatorial attacks also verified and the results confirm that the proposed method is highly robust. This experimental result implies that the proposed method is resistant to different categories of attacks.

It is very clear from Table 7 that the computational complexity of the proposed WHT based watermarking scheme achieves low computational complexity than the other existing methods.

5. Conclusion

The color image watermark is hidden into the color host image using the WHT based watermarking scheme is proposed in this paper. The proposed WHT scheme embeds the data in the third and fourth-row WHT coefficients. The difference and average value of the third and fourth-row WHT coefficients are calculated to extract the embedded data. Besides, the security of information is prevented using the key by shuffling and rearranging the pixel values. The outcome of the proposed method is superior with respect to embedding capacity of 0.25 bpp, visual quality and NC than the conventional watermarking techniques. This watermarking scheme reveals strong robustness against several manipulation and combinatorial attacks.

Conflict of interest

No Conflict of Interest.

Acknowledgments

This research work is partially funded by State Government Ph. D. fellowship, Department of Collegiate Education, Chennai, Tamil Nadu State.

References

- Ansari, I.A., Pant, M., 2017. Multipurpose image watermarking in the domain of DWT based on SVD and ABC. *Pattern Recogn. Lett.* 94, 228–236. <https://doi.org/10.1016/j.patrec.2016.12.010>.
- Araghi, T.K., Manaf, A.B.A., Zamani, M., Araghi, S.K., 2016. A survey on digital image watermarking techniques in spatial and transform domains. *Int. J. Adv. Image Process. Tech.* 3, 6–10.

- Bhatnagar, G., Raman, B., Wu, Q.M.J., 2012. Robust watermarking using fractional wavelet packet transform. *IET Image Process.* 6, 386–397. <https://doi.org/10.1049/iet-ipr.2010.0400>.
- Chung, K.-L., Huang, Y.-H., Chang, P.-C., Liao, H.-Y.M., 2010. Reversible data hiding-based approach for intra-frame error concealment in H. 264 / AVC. *IEEE Trans. Circuits Syst. Video Technol.* 20, 1643–1647. <https://doi.org/10.1016/j.jvcir.2013.12.008>.
- CVG – UGR – Image database [WWW Document], n.d. URL: <http://decmai.ugr.es/cvg/dbimages/c512.php> (accessed 9.24.19).
- Fallahpour, M., 2008. Reversible image data hiding based on gradient adjusted prediction. *IEICE Electron. Express* 5, 870–876. <https://doi.org/10.1587/eleex.5.870>.
- Ganic, E., Eskicioglu, A.M., 2004. Robust DWT-SVD domain image watermarking. In: *Proc. 2004 Multimed. Secur. Work. Multimed. Secur. – MM&Sec '04*, pp. 166–174. <https://doi.org/10.1145/1022431.1022461>.
- Guo, J.M., Prasetyo, H., 2014. False-positive-free SVD-based image watermarking. *J. Vis. Commun. Image Represent.* 25, 1149–1163. <https://doi.org/10.1016/j.jvcir.2014.03.012>.
- Hamidi, M., Haziti, M., El, Cherifi, H., El Hassouni, M., 2018. Hybrid blind robust image watermarking technique based on DFT-DCT and Arnold transform. *Multimed. Tools Appl.* 77, 27181–27214. <https://doi.org/10.1007/s11042-018-5913-9>.
- Hong, G., Huang, Y.-H., Chang, C.-C., Liu, Y., 2014. (k, n)-image reversible data hiding. *J. Inf. Hiding Multimed. Signal Process.* 5, 152–164.
- Jia, S., 2014. A novel blind color images watermarking based on SVD. *Optik (Stuttg.)* 125, 2868–2874. <https://doi.org/10.1016/j.jiloe.2014.01.002>.
- Kalra, G.S., Talwar, R., Sadawarti, H., 2015. Adaptive digital image watermarking for color images in frequency domain. *Multimed. Tools Appl.* 74, 6849–6869. <https://doi.org/10.1007/s11042-014-1932-3>.
- Liu, H., Liu, J., Zhao, M., 2018. Visual saliency model-based image watermarking with Laplacian distribution. *Inf.* 9, 1–13. <https://doi.org/10.3390/info9090239>.
- Meenakshi, K., Rao, C.S., Satya Prasad, K., 2014. A robust watermarking scheme based Walsh-Hadamard Transform and SVD using ZIG ZAG Scanning. In: *Proceedings – 13th International Conference on Information Technology, ICIT 2014*, pp. 167–172. <https://doi.org/10.1109/ICIT.2014.53>.
- Mehto, A., Mehra, N., 2016. Adaptive lossless medical image watermarking algorithm based on DCT & DWT. *Procedia Comput. Sci.*, 88–94. <https://doi.org/10.1016/j.procs.2016.02.015>.
- Ni, Z., Shi, Y.-Q., Ansari, N., Su, W., 2006. Reversible data hiding. *IEEE Trans. Circuits Syst. Video Technol.* 16, 354–362. <https://doi.org/10.1109/TCSVT.2006.869964>.
- Parashar, P., Singh, R.K., 2014. A survey: digital image watermarking techniques. *Int. J. Signal Process. Image Process. Pattern Recogn.* 7, 111–124. <https://doi.org/10.14257/ijsp.2014.7.6.10>.
- Roy, S., Pal, A.K., 2018. An SVD based location specific robust color image watermarking scheme using RDWT and arnold scrambling. *Wirel. Pers. Commun.* 98, 2223–2250. <https://doi.org/10.1007/s11277-017-4971-z>.
- Singh, A.K., 2017. Improved hybrid algorithm for robust and imperceptible multiple watermarking using digital images. *Multimed. Tools Appl.* 76, 8881–8900. <https://doi.org/10.1007/s11042-016-3514-z>.
- SIPI Image Database – Misc [WWW Document], n.d. URL: <http://sipi.usc.edu/database/database.php?volume=misc> (accessed 9.24.19).
- Su, Q., Chen, B., 2018. Robust color image watermarking technique in the spatial domain. *Soft Comput.* 22, 91–106. <https://doi.org/10.1007/s00500-017-2489-7>.
- Su, Q., Niu, Y., Liu, X., Zhu, Y., 2012. Embedding color watermarks in color images based on Schur decomposition. *Opt. Commun.* 285, 1792–1802. <https://doi.org/10.1016/j.optcom.2011.12.065>.
- Su, Q., Niu, Y., Wang, G., Jia, S., Yue, J., 2014a. Color image blind watermarking scheme based on QR decomposition. *Signal Process.* 94, 219–235. <https://doi.org/10.1016/j.sigpro.2013.06.025>.
- Su, Q., Niu, Y., Zou, H., Zhao, Y., Yao, T., 2014b. A blind double color image watermarking algorithm based on QR decomposition. *Multimed. Tools Appl.* 72, 987–1009. <https://doi.org/10.1007/s11042-013-1653-z>.
- Su, Q., Wang, G., Zhang, X., Lv, G., Chen, B., 2018. A new algorithm of blind color image watermarking based on LU decomposition. *Multimed. Syst. Signal Process.* 29, 1055–1074. <https://doi.org/10.1007/s11045-017-0487-7>.
- Su, Q., Zhang, X., Wang, G., 2019. An improved watermarking algorithm for color image using Schur decomposition. *Soft Comput.* <https://doi.org/10.1007/s00500-019-03924-5>.
- Tian, J., 2003. Reversible data embedding using a difference expansion. *IEEE Trans. Circuits Syst. Video Technol.* 13, 890–896. <https://doi.org/10.1109/TCSVT.2003.815962>.
- Walsh-Hadamard Transform – MATLAB & Simulink – MathWorks India [WWW Document], n.d. URL: <https://in.mathworks.com/help/signal/ug/walshhadamard-transform.html> (accessed 1.25.20).
- Xiang-yang, W., Chun-peng, W., Hong-ying, Y., Pan-pan, N., 2012. A robust blind color image watermarking in quaternion Fourier transform domain. *J. Syst. Softw.* <https://doi.org/10.1016/j.jss.2012.08.015>.
- Yen, C.T., Huang, Y.J., 2016. Frequency domain digital watermark recognition using image code sequences with a back-propagation neural network. *Multimed. Tools Appl.* 75, 9745–9755. <https://doi.org/10.1007/s11042-015-2718-y>.